From: Quantum Well and Supelattice Physics V, G.H. Döhler, E.S. Koteles, Eds.,
Proc. SPIE 2139, pp. ~~27-36~~ 331-341 (1994).

(75)

# Free-electron laser nonlinear spectroscopy of doubly resonant (5.5–3.0 μm and 4.1–2.1 μm) InGaAs/AlGaAs asymmetric quantum wells

E.L. Martinet, G.L. Woods, H.C. Chui, J.S. Harris, Jr., M.M. Fejer

Center for Nonlinear Optical Materials, Stanford University, McCullough 226, Stanford CA 94305-4055

C.A. Rella, B.A. Richman

SCA/FEL Free Electron Laser Center, Stanford University, Stanford CA 94305-4085

## 1. ABSTRACT

Conduction band intersubband absorption and second harmonic generation (SHG) are demonstrated in doubly resonant asymmetric step high indium content quantum wells (QW) grown on a GaAs substrate. Intersubband absorption peaks at 5.51 μm and 3.05 μm corresponding to the 1 to 2 and 1 to 3 transitions are measured. The susceptibility of SHG from the QW, $\chi^{(2)}_{QW}$, is measured using a free electron laser by interference between the SHG fields generated from the QW and the GaAs substrate. A large asymmetry in the SHG power with rotation angle of the sample arising from $\chi^{(2)}_{QW}$ is observed. The magnitude and phase of $\chi^{(2)}_{QW}$ is measured in the 4.6–6.3 μm pump wavelength range. $\chi^{(2)}_{QW}$ is of maximum amplitude at 6.0 μm with a value of 145±20 nm/V. A change in the sign of the phase of $\chi^{(2)}_{QW}$ within the SHG resonance is demonstrated for the first time. Agreement of both the linear and nonlinear properties to a simple model assuming lorentzian linewidths is discussed. SHG of 2.0 μm light is also demonstrated in coupled $In_{0.60}Ga_{0.40}As$/AlAs quantum wells.

## 2. HIGH INDIUM CONTENT InGaAs/AlGaAs QUANTUM WELLS

Nonlinear effects from QW intersubband transitions have been widely demonstrated,[1,2] showing much larger susceptibilities than bulk media due to low effective mass and resonance effects. These transitions, however, are typically limited by the conduction band offsets available in QW material systems to the far and mid-infrared (wavelengths longer than 4.5 μm). If shorter wavelength intersubband transitions can be achieved, then applications such as frequency conversion[3] or electro-optic switching[4] should be possible at technologically important wavelengths (2 μm or 1.5 μm) where laser diodes are available.[5]

Until recently, intersubband phenomena in the 1.8–5 μm IR regime have remained largely unexplored because of both the lack of semiconductor materials presenting sufficient bandgap engineering possibilities and the difficulty in obtaining tunable high power sources in this wavelength region. The introduction of high indium content InGaAs/AlGaAs QWs[6,7], together with the development of free-electron laser (FEL) facilities,[8] uncover a new field of experiments in that wavelength range. Strained InGaAs/AlGaAs QWs grown on GaAs have very large conduction band offsets (up to 1.4 eV) and low effective mass and thus may yield both larger intersubband transition energies and larger $\chi^{(2)}_{QW}$ than GaAs/AlGaAs QWs.[9,10] However, InGaAs/AlGaAs QWs are highly strained and difficult to grow. We have recently demonstrated high indium content InGaAs/AlGaAs QWs with intersubband transition resonances out to 2.1 μm.[10–12] This was made possible by reducing epilayer strain with a graded InGaAs buffer.[6,13] The buffer acts as an effective substrate with a lattice constant corresponding to the InGaAs on top of the buffer (see figure 1), the composition of which is chosen to balance the strain between the QW barrier and well materials. This enables one to increase the range of bandgap engineering to highly strained (up to at least 65% In) systems in order to design a well geometry that optimizes the linear or nonlinear susceptibilities of the system at a given transition energy. However, the nonlinear properties from these short wavelength intersubband transitions have yet to be investigated. In this work, we investigate the $\chi^{(2)}_{QW}$ of high indium content doubly resonant (5.5–3.0 μm and 4.1–2.1 μm) asymmetric multi-QWs (MQWs) using a FEL.

0-8194-1434-4/94/$6.00

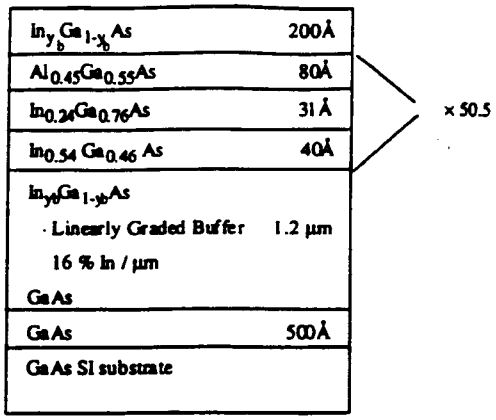


**Figure 1.**
Layer structure for the high indium content (54%) multi-QW sample used in this study. The graded InGaAs buffer final In composition is $y_b$=19%.

## 3. QUANTUM WELL OPTIMIZATION FOR MAXIMUM SHG

The magnitude of the intersubband susceptibility for a QW in a simple perturbative model is governed by the magnitude of the dipole moments, the energies and linewidths of the transitions.[14] We have previously demonstrated that the transition energies and dipole moments for high indium content InGaAs/AlGaAs square QWs can be modeled with a single band effective mass model, taking nonparabolicity into account by using an energy dependent effective mass.[10–12] We assume a lorentzian fit to the linear absorption, with a linear susceptibility $\chi^{(1)}_{QW}$, due to the QW:

$$\chi^{(1)}_{QW}(\omega) = \frac{q^2\sigma_1}{\varepsilon_0 L_{QW}} \sum_n \frac{|z_{1n}|^2}{(\hbar\omega - E_{1n} - i\Gamma_{1n})} \tag{1}$$

where $z_{mn}$ are dipole matrix elements of the transition between the $m^{th}$ and $n^{th}$ QW envelope states, $E_{mn}$ are the intersubband energies and $\Gamma_{mn}$ are the half width half maximum (HWHM) lorentzian linewidths. We assume that only the ground level is populated with a sheet carrier density $\sigma_1$ per QW period $L_{QW}$. We want now to investigate whether the same simple perturbative model can be applied to $\chi^{(2)}_{QW}$. Optical spectroscopy of both the linear and nonlinear response is used to investigate this model in asymmetric QWs which have been optimized for maximum $\chi^{(2)}_{QW}$. Because the absorption losses from $\chi^{(1)}_{QW}$ are present close to the $\chi^{(2)}_{QW}$ maxima, these spectra must be known accurately in order to calculate the figure of merit of any device.[3]

### 3.1 Doubly resonant asymmetric QW

SHG in *n*–type QWs has been reported in the 10 µm region,[1–2] in which the symmetry is broken by applying an electrical bias across a square well[15] or growing compositionally asymmetric QWs (step wells[16–18] or coupled[9] QWs for example). The $\chi^{(2)}_{QW}$ can be approximated in that case as:[19]

$$\chi^{(2)}_{QW}(\omega) = \frac{q^3\sigma_1}{\varepsilon_0 L_{QW}} \sum_{m,n} \frac{z_{1n}\, z_{nm}\, z_{m1}}{(\hbar\omega - E_{1n} - i\Gamma_{1n})(2\hbar\omega - E_{1m} - i\Gamma_{1m})} \tag{2}$$

Nearly doubly resonant quantum wells with $E_{12} \sim E_{23}$ were reported to yield the highest SHG susceptibility,[16–18] for which the dominant term of $\chi^{(2)}_{QW}$ is:

$$\chi^{(2)}_{QW\ peak}(\omega) \propto \frac{z_{12}\, z_{23}\, z_{31}}{(\hbar\omega - E_{12} - i\,\Gamma_{12})\,(2\,\hbar\omega - E_{13} - i\,\Gamma_{13})} \tag{3}$$

The design of a QW to produce maximum $\chi^{(2)}_{QW}$ consists of achieving both a maximum dipole matrix element product, $z_{12} \times z_{23} \times z_{31}$ by optimizing the well shape, together with a minimum in the denominator. The latter consideration consists of achieving double resonance and minimum linewidths for a given targeted transition energy. This can be done by adjusting the growth parameters.[13]

### 3.2 Sample description

The asymmetric step MQW structure used in this study was designed to have a near double resonance with the maximum $\chi^{(2)}_{QW}$ at 5.3 μm. The intersubband absorption was modeled with a single band effective mass model as described above. The sample was grown by molecular beam epitaxy on a (100) GaAs wafer, using an InGaAs graded buffer.[6] The asymmetric step QW structure consists of 50 periods of 40 Å $In_{0.54}Ga_{0.46}As$ and 31 Å $In_{0.24}Ga_{0.76}As$ QWs separated by 80 Å $Al_{0.45}Ga_{0.55}As$ barriers, resulting in a QW period $L_{QW}$ = 151 Å, as shown in figure 2.

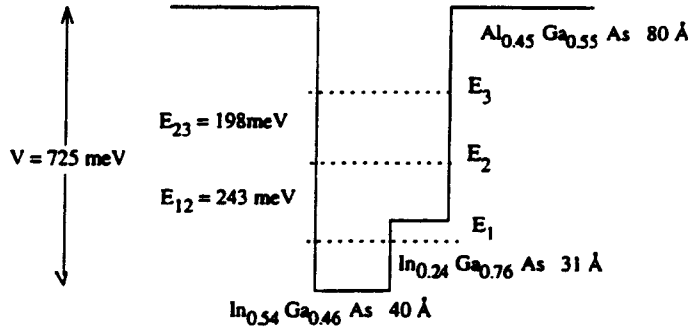


**Figure 2.**
Conduction band diagram and calculated eigenenergies of the asymmetric step QWs used in this study.

The quantum well was *n*–doped in the high indium section of the well, resulting in a measured Hall sheet charge density of $\sigma_1 = 2.94 \times 10^{12}$ cm$^{-2}$ per QW. The maximum conduction band discontinuity was 725 meV (1.7μm). The calculated intersubband transition energies and dipole moments were $E_{12}$ = 243 meV (5.1 μm), $E_{13}$ = 441 meV (2.8 μm), $z_{12}$ = 16.38 Å, $z_{13}$ = –2.52 Å, $z_{23}$ = 19.33 Å, $z_{22}-z_{11}$ = 11.86 Å, $z_{33}-z_{11}$ = 7.80 Å. A linearly graded InGaAs buffer with a final composition of 19% In was used to provide strain compensation.[6,13] The sample was grown using $As_4$ at a substrate temperature of 430°C. The indium buffer and QW compositions were determined by high resolution x-ray diffraction on a reference sample with thick, relaxed InGaAs grown under the same conditions.

### 3.3 Linear spectrum and calculation of $\chi^{(2)}_{QW}$ of the MQW structure

The absorption spectrum of the structure was measured using an FTIR spectrometer, with the sample mounted at Brewster's incidence angle to TM polarized light. A proton bombarded sample was used as a reference to compensate for multiple reflection effects from the MQW epilayer.[18] The absorption spectrum is shown in figure 3. An absorption peak corresponding to the 1 to 2 transition at 225 meV (5.51μm) with a HWHM of 13 meV and integrated absorption fraction (IAF) of 26.6 mAbs-meV-per-QW is observed. A smaller feature corresponding to the 1 to 3 transition is also seen at 407 meV (3.05 μm) with a HWHM of 23 meV and an IAF of 3.13 mAbs-meV-per-QW. The measured intersubband energies are within 10% of the theoretically predicted values. One can note that the 1 to 2 transition is resonant at 5.5 μm and the 1 to 3 at 3 μm which means that the double resonance criterion is only approximate for this structure. The best lorentzian fits to the absorption peaks shown in figure 3 yield intersubband energies of $E_{12}$ = 225 meV and $E_{13}$ = 409 meV and linewidths of $\Gamma_{12}$ = 11 meV and $\Gamma_{13}$ = 22meV for the transitions 1 to 2 and 1 to 3, respectively. Assuming $z_{12}$ = 16.4Å

from theory, the measured IAFs yield an effective doping concentration of $\sigma_1 = (1.6\pm0.2)\times10^{12}$ cm$^{-2}$ per QW and $z_{13}$ = 4.21Å. This $z_{13}$ is 1.7 times the calculated value. Simple calculations indicate that these discrepancies could be taken into account by adding band bending effects to the simple model that we used to calculate the transition energies and dipole moments.

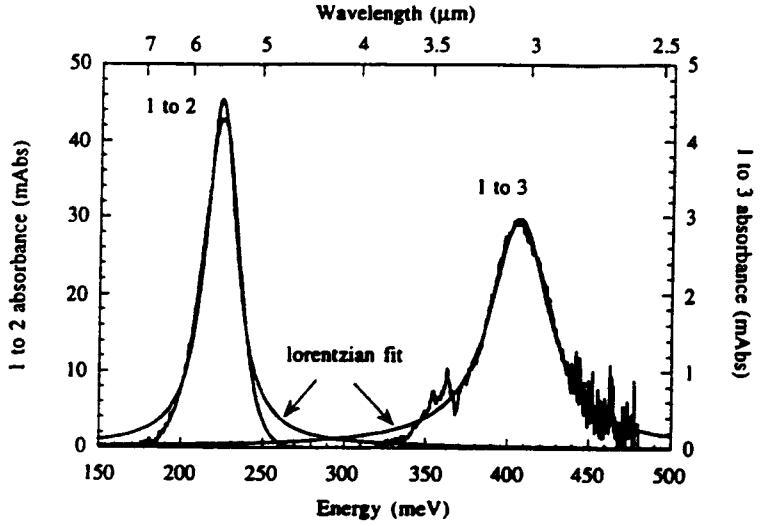


**Figure 3.**
Absorption spectrum of the step quantum well sample and best lorentzian fits.

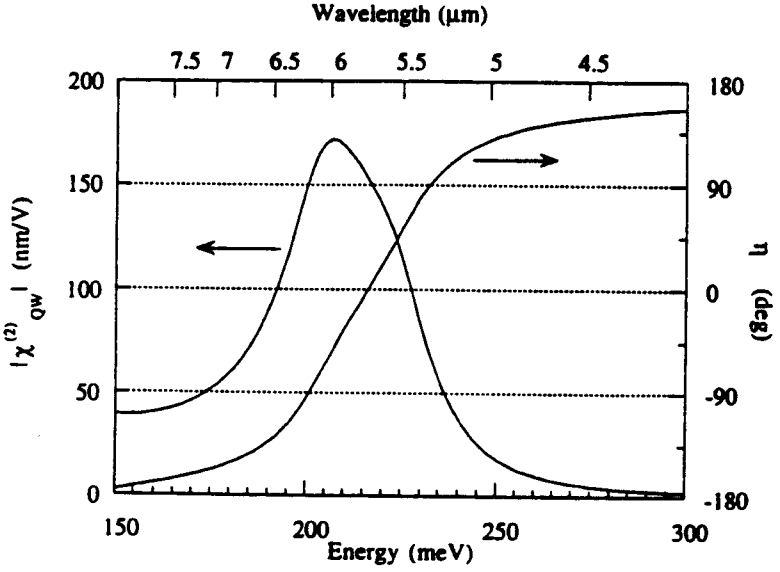


**Figure 4.**
Calculated magnitude and phase of the $\chi^{(2)}_{QW}$ from the asymmetric step QW

The $\chi^{(2)}_{QW}$ can be calculated by treating the QW as a 3 level system. Assuming lorentzian lineshapes for the transitions, the $\chi^{(2)}_{QW}$ is then given by eqn. (2). Using the intersubband transition parameters derived from absorption measurements, and assuming $z_{23}$ = 19.3 Å and $z_{22}$–$z_{11}$ = 11.6 Å from theory, an estimate for the magnitude and phase $\eta(\omega)$ of the $\chi^{(2)}_{QW}$ is obtained and shown in figure 4. The $\chi^{(2)}_{QW}$ is maximum at 6 μm as compared to the 5.5 μm absorption peak because the double resonance is only approximate. The calculated magnitude of $\chi^{(2)}_{QW}$ using the absorption data is 170 nm/V, nearly 1000 times larger than the $\chi^{(2)}_{QW}$ of bulk GaAs (0.18 nm/V),[20] already a good nonlinear material.

## 4. PHASE RESOLVED SPECTROSCOPY OF $\chi^{(2)}_{QW}$

### 4.1 Nonlinear interference spectroscopy

For the QW structure grown on GaAs, both the epilayer ($\chi^{(2)}_{QW}$) and the substrate ($\chi^{(2)}_{GaAs}$) are sources of SHG. The extraction of $\chi^{(2)}_{QW}$ makes use of the interference between the GaAs and multilayer generated second harmonic electric fields.[19, 21, 22] Figure 5 shows the electric field coupling configuration to the sample. The incident light —described by the electric field $E(\omega)$— enters the sample with an incidence angle, $\vartheta$, (internal angle $r$), and an angle $\varphi$ between the (110) direction of the GaAs substrate and the plane determined by the direction (001) and the polarization of the incident electric field, as shown. A harmonic electric field $E(2\omega)$ builds up from the QW epilayer over a length $L_{MQW}$ (= 0.6 μm), with a phase $\eta(\omega)$. The substrate of thickness $L$ is many coherence lengths long ($l_C$ is a few tens of microns in the mid IR). The GaAs substrate generated electric field builds up over the last fractional coherence length, $l_C \times \sin \zeta$, where $\zeta$ is the phase shift between $E(\omega)$ and $E(2\omega)$ after a length $L$. The SHG signal measured after the sample is given by the coherent superposition of these two fields.

For comparable values of the susceptibilities $\chi^{(2)}_{GaAs}$ and $\chi^{(2)}_{QW}$, the SHG signal from the bulk overwhelms that of the epilayer, by a factor given by the ratio of the square of the lengths in which the radiation is generated. However, the symmetry and electronic structures of the bulk and epilayer region are different: $\chi^{(2)}_{GaAs}$ and $\chi^{(2)}_{QW}$ have different non-zero elements, *(xyz)* and *(zzz)* respectively, so that polarization selection leads to measurement of either a coherent superposition signal or only the GaAs generated signal. Assuming that $\zeta$ is known, we can thus extract both the magnitude and the phase $\eta(\omega)$ of $\chi^{(2)}_{QW}$. Considering only the TM polarization of both $E(\omega)$ and $E(2\omega)$, the SHG conversion can be expressed as:[3]

$$\frac{I_{2\omega}}{I_{\omega}^2} = T(\vartheta)\left| \chi^{(2)}_{GaAs} \frac{l_c \cos r}{\pi} G_{xyz}(r,\varphi) \times \left(e^{+2i\zeta} - 1\right) + \chi^{(2)}_{QW}(\omega) L_{MQW} F_{zzz}(r) \right|^2 \tag{4}$$

where $I_{2\omega}$ and $I_{\omega}$ are the harmonic and fundamental power densities. $T(\vartheta) = | t_{\omega}^2(\vartheta)\, t'_{2\omega}(\vartheta) |^2$, where $t_{\omega}(\vartheta)$ and $t'_{2\omega}(\vartheta)$ are the electric field transmission coefficients from air to GaAs for the pump and GaAs to air for the second harmonic. $G_{xyz} = 3\cos^2 r \sin r \cos 2\varphi$, and $F_{zzz} = \sin^3 r$ are the projection of electric fields on the principal axes of the crystal. The phase difference, $\zeta$, between the $\omega$ and $2\omega$ electric fields after the sample, can be expressed as:

$$\zeta = \frac{\pi}{2} \frac{L}{l_c \cos r} \tag{5}$$

where $l_C$ is the coherence length for the interaction, defined in terms of the bulk dispersion by:

$$l_c = \frac{\pi c}{2\omega (n_{2\omega} - n_{\omega})} \tag{6}$$

where $n_{\omega}$ and $n_{2\omega}$ are the refractive indices at the fundamental and second harmonic frequencies.

The extraction of $\chi^{(2)}_{QW}$ consists of measuring the SHG signal for different polarization configurations and then fitting equation (4) with $\chi^{(2)}_{QW}$, as the only (complex) parameter. This provides both amplitude and phase information if the phase difference, $\zeta$, is known with sufficient accuracy. The value of the coherence length is either calculated from the measured value of the GaAs indices in the mid–infrared according to eqn. (6)[23] or directly measured using a Maker fringe method.[19,24]

### 4.2 Coherence length measurements

The sample length was measured either directly or through etalon effects in the absorption spectrum to be $L = 514\pm5$ μm, on the order of 10 coherence lengths thick. Thus phase–resolved spectroscopy requires knowledge of $l_c$ to a few percent accuracy in order to measure $\eta(\omega)$ within less than 10% of the $2\pi$ phase range. Calculated values of $l_c$ can be obtained via eqn. (6) using the published values of the refractive index for GaAs.[23] Assuming an accuracy of $10^{-3}$ on the indices, one obtains $l_c$ = 71±10 μm at 6 μm, which is not sufficiently accurate. We therefore measured the coherence length using a wedge Maker-fringe technique[19,24] and obtained $l_c = 44.7\pm2.1$ μm at $\lambda = 5.19$ μm and $l_c = 52.7\pm1.8$ μm at $\lambda = 4.8$ μm (using eqn. (6), we calculated 43.7±5.6 μm and 52.7±3.8 μm at 5.19 and 4.8 μm, respectively). The dispersion of $l_c$ was modeled via eqn. (6) using the published values of the refractive index for GaAs ,[23] with a constant offset chosen to yield agreement with our direct measurement.

### 4.3 Free-electron laser experimental arrangement

SHG measurements were performed with a free electron laser (FEL). The Stanford SCA/FEL[8] generates pulses with micropulse length of about 2 picoseconds and a peak power a few 100s of kW, and is tunable between 3.5 and 6.5μm. The pump beam is focused onto the sample with a focal spot of 100 μm diameter. Filters are placed both before and after the sample in order to block the incident second harmonic radiation from the FEL and to block the pump radiation after the sample, as shown in figure 6. ZnSe polarizers are used on both the input and collection side to select only the TM polarization for the sample. An InSb or PbS detector was used to measure the SHG signal. In addition, a pick-off from the FEL pump beam was focused onto a properly phase matched $AgGaSe_2$ crystal and detected with an InSb detector for use as a reference SHG signal. The measured SHG power was then normalized to fluctuations in the pump power by dividing by the reference SHG signal or the square of the measured fundamental power. The QW sample was placed on a rotation stage which allowed for variations of the incidence angle $\vartheta$ and rotations about the sample normal (figure 5). A proton bombarded QW sample —where no carriers are available for excitation so that $\chi^{(2)}_{QW}$ is null[18]— was used to determine the substrate contribution. The latter sample provides a normalization of the susceptibilities to that of GaAs.

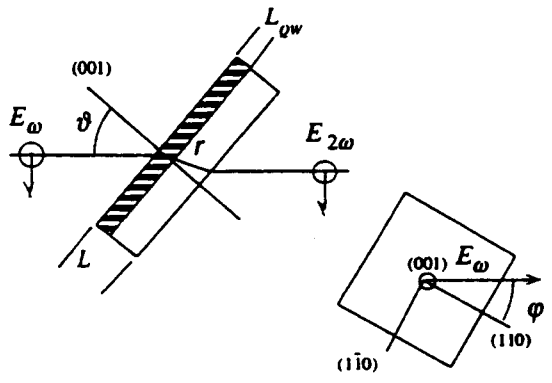


**Figure 5.**
Electric field coupling to the sample.

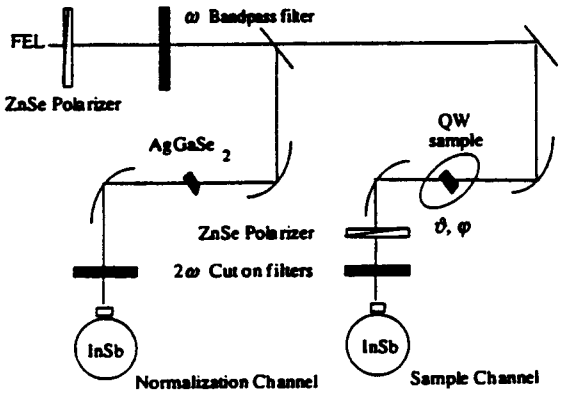


**Figure 6.**
Experimental setup.

### 4.4 Discussion of the nonlinear spectra obtained from rotation of the sample about its normal

Figures 7 and 8 show typical scans obtained when $\varphi$ is varied on the proton bombarded reference and QW samples respectively. The scan were performed with a 6.26 μm wavelength pump and an incidence angle $\vartheta = 45°$. According to eqn. (4), as the angle $\varphi$ is varied, the SHG from a proton bombarded sample yields 4 even peaks following a $G_{xyz}{}^2(r, \varphi) \propto \cos^2 2\varphi$ dependence. This arises from the pure GaAs contribution, as seen in figure 7. A best fit to the experimental data is given as well. Figure 8 shows the variation of the SHG power with $\varphi$ arising from the QW sample. Two features are noted: (1) an unevenness between the 0°, 180° peaks and the 90°, 270° peaks, and (2) a DC baseline of the SHG. These features are due to the $\varphi$–independent QW term superposed with the GaAs one. Eqn. (4) can be written as:

$$\frac{I_{2\omega}}{I_{\omega}^2}(\varphi) \propto \left| \chi^{(2)}_{GaAs} \cos(2\varphi) \times \sin(\zeta)\, e^{+i\zeta} + f_{\omega} \left| \chi^{(2)}_{QW}(\omega) \right| \times e^{+i\eta(\omega)} \right|^2 \tag{7}$$

where $f_{\omega}$ is the ratio of the effective interaction lengths of the QW to that of the GaAs substrate. The asymmetry between the peaks(1) and the DC offset (2) of the φ scan are due to:

$$\frac{\left| \chi^{(2)}_{QW}(\omega) \right|}{\chi^{(2)}_{GaAs}} \cos(\eta(\omega) - \zeta) \tag{8}$$

and

$$\frac{\left| \chi^{(2)}_{QW}(\omega) \right|}{\chi^{(2)}_{GaAs}} \left| \sin(\eta(\omega) - \zeta) \right|, \tag{9}$$

respectively. A fit of the $\varphi$ scan from the QW sample leads to the values of the $\chi^{(2)}{}_{QW}$, in phase and in quadrature with the bulk contribution. The best fit of the $\varphi$ scan is shown in figure 8, where the only two fitting parameters are the imaginary and real part of $\chi^{(2)}{}_{QW}$. Usually, $f_{\omega}$ is of the order of $10^{-3}$ so $E(2\omega)$ arising from the GaAs is larger than that of the QW due to a better effective coupling of the light and a greater interaction length. Thus the cross term (8) of first order compared with the SHG from the proton bombarded sample and the pure QW term (9) is of second order, for which the signal to noise ratio is poorer.

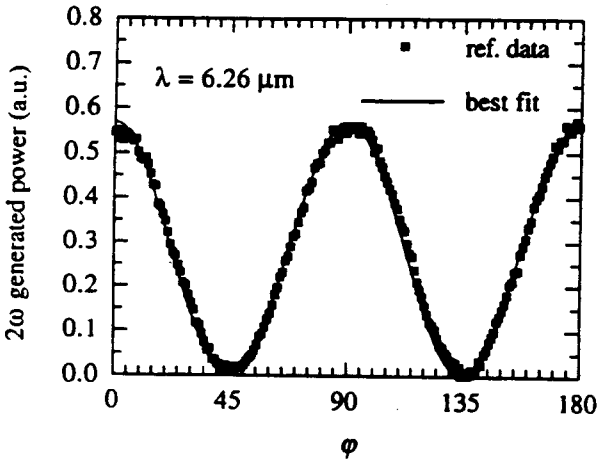


**Figure 7.**
Variation of the SHG power as a function of $\varphi$ angle for the proton bombarded sample at $\lambda = 6.26$ μm

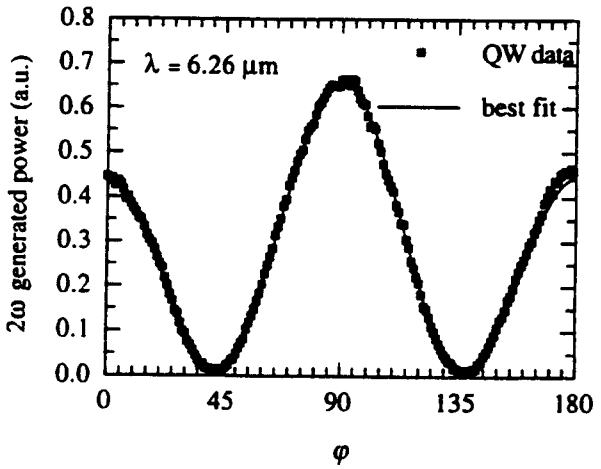


**Figure 8.**
Variation of the SHG power as a function of $\varphi$ angle for the QW sample at $\lambda = 6.26$ μm

As an example, the 6.26 μm wavelength has been chosen so that the SHG signal generated from the GaAs is a maximum: $l_c = 77.1$ μm, so that $\zeta = -1.06 \times \pi/2$. In this case, the DC offset results from the real part, and the asymmetry of the peaks, from the imaginary part of the $\chi^{(2)}{}_{QW}$. We measured a $\chi^{(2)}{}_{QW}$ of real part −123±50 nm/V and imaginary part −52±23 nm/V,

intersubband absorption spectrum for the QWs is shown in figure 11. Two absorption peaks are seen at 295 meV (4.1 μm) and 580 meV (2.1 μm). Lorentzian lineshapes fit to the absorption peaks yielded HWHM linewidths of $\Gamma_{12} = 41$ meV and $\Gamma_{13} = 67$ meV and IAFs of 28.0 and 9.8 mAbs-meV-per-QW for the 1 to 2 and 1 to 3 transitions, respectively. The $\chi^{(2)}_{QW}$ estimated from perturbation theory is 12 nm/V. SHG measurements were performed with the FEL tuned to a wavelength of 4.0 μm. A large asymmetry with respect to rotation of the sample is observed, arising from the SHG from the QW, and a $\chi^{(2)}_{QW}$ of magnitude 22±6 nm/V was measured, 110 times larger than the bulk GaAs $\chi^{(2)}$.[26]

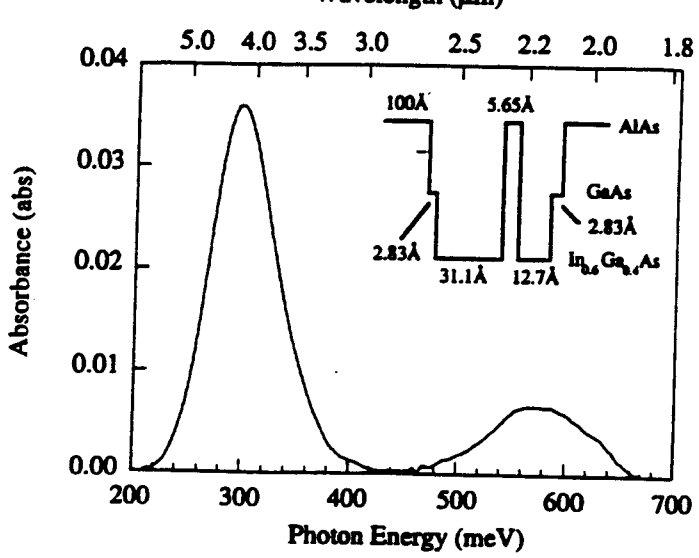


**Figure 11.**
Intersubband absorption spectrum for doubly resonant asymmetric coupled $In_{0.6}Ga_{0.4}As$/ AlAs QWs with conduction band diagram (insert).

## 6. CONCLUSIONS

Second harmonic generation in the mid-IR from high indium content InGaAs/AlGaAs QWs grown on a GaAs substrate is demonstrated. Linear and nonlinear spectroscopy of a doubly resonant asymmetric step QW susceptibility was performed. The magnitude and phase of the $\chi^{(2)}_{QW}$ was measured by interfering the SHG field from the QWs and GaAs substrate. The magnitude of the $\chi^{(2)}_{QW}$ is 145±20 nm/V for 3 μm generated light. A phase change within the resonance of the $\chi^{(2)}_{QW}$ was demonstrated for the first time by a sign change of the spectrum of the imaginary component of the $\chi^{(2)}_{QW}$. Qualitative agreement of the linear and nonlinear spectra with a simple model was found. Doubly resonant generation of 2.0 μm light in a coupled $In_{0.6}Ga_{0.4}As$/AlAs was also performed, and a magnitude of $\chi^{(2)}_{QW}$ of 22±6 nm/V was measured. This is the shortest wavelength SHG demonstrated in an *n*–type QW. These large nonlinear susceptibilities may result in efficient nonlinear optical conversion and electro-optic switching devices[3,4] in the technologically important 2 μm wavelength range where diode laser sources are available.[5]

## 7. ACKNOWLEDGMENTS

E.L. Martinet acknowledges fellowship support from the Office of Naval Research (ONR) and Lockheed, G.L. Woods from the Center for Nonlinear Optical Materials (CNOM), and H.C. Chui from an ONR Fellowship. This work was supported by ONR under contract N00014-91-J-0170 and N00014-92-J-1903, by ARPA under contract N00014-90-J-4056 and CNOM under contract number N00014–92–J–1903. FTIR measurements were performed on a Bruker FTIR at the Stanford Free Electron Laser facility.

## 8. REFERENCES


1. Bibliography: NATO ASI Intersubband Transitions in Quantum Wells, E.Rosencher, B. Vinter, B. Levine, eds., vol. 288, Plenum, New York, 1992.

2. Bibliography: NATO ASI Quantum Well Intersubband Transition Physics and Devices, H.C. Liu, B.F. Levine, J.Y. Andersson, eds., Kluwer Academic Publishers, to be published, 1994.

3. S.B.J. Yoo, "Linear and Nonlinear Spectroscopy of Quantum Well Intersubband Transitions," *Ph.D. Thesis*, Stanford University, 1991.

4. J. Khurgin, "Second-order intersubband nonlinear-optical susceptibilities of asymmetric quantum-well structures," *J. Opt. Soc. Am. B*, Vol. 6(9), pp. 1673-82, 1989.

5. H.K. Choi, S.J. Eglash, M.K. Connors, "Single frequency GaInAsSb/AlGaAsSb quantum-well ridge-waveguide laser emitting at 2.1 μm," *Appl. Phys. Lett.*, 63(24), pp. 3271–2, 1993.

6. S.M. Lord, B. Pezeshki, J.S. Harris, Jr., "Investigation of High In Content InGaAs Quantum Wells Grown on GaAs by Molecular Beam Epitaxy," *Electronics Letters*, 28 (13), pp.1193–1195, 1992.

7. Y. Hirayama, J.H. Smet, L.H. Peng, C.G. Fondstad, E.P. Ippen, "Observation of 1.798 μm intersubband transition in InGaAs/AlAs pseudomorphic quantum well heterostructure," *Appl. Phys. Lett.*, 63(12), pp. 1663–5, 1993.

8. T.I. Smith, H.A. Schwettman, K.W. Berryman, R.L. Swent, "Facilities at the Stanford Picosecond FEL Center," in: SPIE Proceedings, H.A. Schwettman, ed.:*Free Electron Laser spectroscopy in Biology, Medicine, and Material Science*, Vol. 1854, pp. 23–33, Los Angeles, 1993.

9. F. Capasso, C. Sirtori, D. Sivco, A.Y. Cho, "Nonlinear Optics of Intersubband Transitions in AlInAs/GaInAs Coupled Quantum Wells: Second Harmonic Generation and Resonant Stark Tuning of $\chi_{2\omega}^{(2)}$," in: NATO ASI Intersubband Transitions in Quantum Wells, E. Rosencher, B. Vinter, B. Levine, eds., Vol. 288, pp. 141-9, Plenum, New York, 1992.

10. H.C. Chui, S.M. Lord, E. Martinet, M.M. Fejer, J.S. Harris, Jr., "Intersubband transitions in high indium content InGaAs/AlGaAs quantum wells," *Appl. Phys. Lett.*, 63(3), pp.364–6, 1993.

11. H.C. Chui, E.L. Martinet, M.M. Fejer, J.S. Harris, Jr., "Short wavelength intersubband transitions in InGaAs /AlGaAs quantum wells," To be published in *Appl. Phys. Lett.*, 64(6), 1994.

12. H.C. Chui, E.L. Martinet, M.M. Fejer, J.S. Harris, Jr., "Large energy intersubband transitions in high Indium content InGaAs /AlGaAs quantum wells", in: NATO ASI Quantum Well Intersubband Transition Physics and Devices, H.C. Liu, B.F. Levine, J.Y. Andersson, eds., Kluwer Academic Publishers, 1994.

13. H.C. Chui, J.S. Harris, Jr., "Growth Studies of $In_{0.5}Ga_{0.5}As$/AlGaAs Quantum Wells Grown on GaAs with a Linearly Graded InGaAs Buffer," to be published in *J. Vac. Sci. Tech. B*, Mar/Apr. issue 1994.

14. L.C. West, S.J. Eglash, "First observation of an extremely large dipole infrared transition within the conduction band of a GaAs quantum well," *Appl. Phys. Lett.*, 46(12), pp. 1156–8, 1985.

15. M.M. Fejer, S.J.B. Yoo, R.L. Byer, A. Harwit, J.S. Harris, Jr., "Observation of extremely large quadratic susceptibility at 9.6–10.8 μm in electric-field-biased quantum wells," *Phys. Rev. Lett.*, 62(9), pp. 1041–4, 1989.

16. E. Rosencher, P. Bois, J. Nagle, S. Delaître, "Second harmonic generation by intersubband transitions in compositionally asymmetrical MQWs," *Electron. Lett.*, 25(16), pp. 1063–5, 1989.

17. P. Boucaud, F.H. Julien, D.D. Yang, J.M. Lourtioz, E. Rosencher, P. Bois, J. Nagle, "Detailed analysis of second harmonic generation near 10.6 μm in GaAs/AlGaAs asymmetric quantum wells," *App. Phys. Lett.*, 57(3), pp. 272–5, 1990.

18. S.J.B. Yoo, M.M. Fejer, R.L. Byer, J.S. Harris, Jr., "Second Order Susceptibility in Asymmetric Quantum Wells and its Control by Proton Bombardment," *Appl. Phys. Lett.*, 58(16), pp. 1724-26, 1991.

19. Y.R. Shen, The Principles of Nonlinear Optics, Wiley, New York, 1984.

20. B.F. Levine, C.G. Bethea, "Non linear susceptibility of GaP: Relative Measurement and Use of Measured Values to Determine a Better Absolute Value," *Appl. Phys. Lett.*, 20(8), pp. 272-5, 1972.

21. J.J. Wynne, N. Bloembergen, "Measurement of the lowest-order nonlinear susceptibility in III-V semiconductors by second-harmonic generation with CO2 laser," *Phys. Rev.*, 188(3), pp. 1211, 1969.

22. R.W.J. Hollering, "Bulk and surface second-harmonic generation in noncentrosymmetric semiconductors," *Optics Comm.*, 90(1-3), pp. 147-50, 1992.

23. A.N. Pikhtin, A.D. Yas'kov, "Dispersion of the refractive index of semiconductors with diamond and zinc-blende structures," *Sov. Phys. Semicond.*, 12(6), pp, 622-6, 1978.

24. S.K. Kurtz, "Measurement of Nonlinear Optical Susceptibilities," in: Quantum electronics Volume I: Nonlinear optics, Part A, Herbert Rabin and C.L. Tang, eds., Chap.3, pp.209-81. Academic Press, New York, 1975.
25. E.L. Martinet, B.J. Vartanian, G.L. Woods, H.C. Chui, M.M. Fejer, J.S. Harris, Jr., C.A. Rella, B.A. Richman, "Applications of high indium content InGaAs /AlGaAs quantum wells in the 2–7 μm regime", in: NATO ASI Quantum Well Intersubband Transition Physics and Devices, H.C. Liu, B.F. Levine, J.Y. Andersson, eds., Kluwer Academic Publishers, 1994.
26. H.C. Chui, "Doubly resonant Second Harmonic Generation of 2.0 μm light in coupled AlAs/InGaAs quantum wells," to be published.